Biosensors and Bioelectronics 45 (2013) 230–236

Contents lists available at SciVerse ScienceDirect

Biosensors and Bioelectronics

journal homepage: www.elsevier.com/locate/bios

A novel surface plasmon resonance biosensor based on graphene oxide decorated with gold nanorod–antibody conjugates for determination of transferrin

Jia Zhang, Ying Sun, Bo Xu, Hua Zhang, Yan Gao, Hanqi Zhang, Daqian Song*

College of Chemistry, Jilin University, Qianjin Street 2699, Changchun 130012, PR China

ARTICLE INFO

Article history:
Received 19 November 2012
Received in revised form
6 February 2013
Accepted 6 February 2013
Available online 16 February 2013

Keywords:
Graphene oxide
Gold nanorod
Surface plasmon resonance
Transferrin

ABSTRACT

A surface plasmon resonance (SPR) biosensor based on graphene oxide (GO) decorated with gold nanorod (AuNR)–antibody conjugates was developed. Compared with traditional SPR biosensor, GO sheets were assembled on the amino-modified Au film via electrostatic interaction, and then AuNR–antibody conjugates were immobilized via carbodiimide-assisted amidation reaction. The abundant oxygen-containing functional groups, large specific surface area and friendly biocompatibility of GO sheets are beneficial to the immobilization of AuNR–antibody conjugates. Meanwhile, AuNRs are anchored to the GO surface through antibody and function as enhancers for the transferrin determination, which greatly enhance the sensitivity of the detection. As a result, the present biosensor shows a satisfactory response to transferrin in the concentration range of 0.0375–40.00 μg mL^{-1}. The lowest concentration of transferrin that can be determined by this method is about 32-fold lower than that obtained with the sensor based on Au film. This design affords a facile method of controlling the assembly of AuNRs on the GO sheets and can be easily extended to other protein detection by preparing corresponding AuNR–antibody conjugates.

1. Introduction

Sensitive detection of disease-related proteins was critical for many biomedical research and diagnostics (Bilitewski 2000). The assay based on the surface plasmon resonance (SPR) has gained considerable momentum and the number of reporting applications has been rapidly growing (Homola, 2008). In recent years, some materials with excellent properties have been proposed to improve the performance of SPR biosensors, such as gold nanoparticles (Lyon et al., 1998; Chang et al., 2011), magnetic nanoparticles (Sun et al., 2007), carbon nanotubes (Hu et al., 2010), and electropolymerized molecularly imprinted polythiophenes (Pernites et al., 2010). Although great achievement has been obtained, it was still a challenge for the fabrication of novel SPR immunosensors using new materials to achieve sensitive, fast and facile detection.

Graphene oxide (GO) is a strongly oxygenated, highly hydrophilic layered material (Boukhvalov and Katsnelson, 2008). Abundant oxygen-containing functional groups on its basal planes and edges enable GO to interact with varieties of biomolecules through covalent, noncovalent or electrostatic interactions (Cai et al., 2011; Q.Y. He et al., 2010;). In addition, its effectiveness in quenching fluorescence affords advantages over alternative carbon materials such as nanodiamonds, and carbon nanotubes that have been investigated for biosensing (Chang et al., 2008; Satishkumar et al., 2007; Loh et al., 2010). Considering its large specific surface area, long-term stability, friendly biocompatibility and exceptional fluorescence-quenching ability, GO-based sensors have been successfully applied to the detection of ss-DNA (Dong et al., 2010), metal ions (Wen et al., 2010), living cells (Q.Y. He et al., 2010; S.J. He et al., 2010) and Salmonella typhi (Singh et al., 2012). The nanostructures of GO–Ag nanoparticles were used as SERS substrates (Ren et al., 2011). A novel electrochemiluminescence sensor based on the CdSe QDs was designed by Wang et al. (2012). However, there have been a few reports exploring GO based immuno-biosensor (Jung et al., 2010). Au is regarded as an excellent material in immunoassay (Daniel and Astruc, 2004). Compared with spherical Au nanoparticles, Au nanorods (AuNRs) exhibit two plasmon resonance wavelengths defined as transverse and longitudinal mode (Parab et al., 2010). The longitudinal band of AuNRs has been found to be very sensitive to changes in the local environment. Therefore, AuNRs are more sensitive for detecting biological molecules than nanoparticles with spherical structure. The system of GO and AuNRs may serve as a new platform for various applications due to the combination of the high loading capacity of GO with the outstanding optical property of AuNRs.

Transferrin is essential for normal cell growth and maintenance. People with acute hepatitis, anemia, and pregnancy are associated with the symptoms of the increased levels of transferrin, while

* Corresponding author. Tel./fax: +86 431 85168399.
E-mail address: songdq@jlu.edu.cn (D. Song).

0956-5663/$ - see front matter © 2013 Elsevier B.V. All rights reserved.
http://dx.doi.org/10.1016/j.bios.2013.02.008

nephritic syndrome, rheumatism, cirrhosis, malignant tumor, and acute leukemia are characterized by the decrease of this carrier (Asobayire et al., 2001; Das and Abbi, 2003). Thus, it is of great essence to detect transferrin in a rapid, accurate and sensitive way (Liu et al., 2006).

Here we report a novel SPR biosensor using GO sheets decorated with AuNR–antibody conjugates substrate. AuNR–antibody conjugates were immobilized on the GO sheets by a carbodiimide-assisted amidation reaction. The high loading capacity and good biocompatibility of GO together with remarkable optical property of AuNRs are beneficial to antibody immobilization and sensitivity enhancement of detection.

2. Experimental

2.1. Materials

Transferrin, rabbit anti-transferrin, human IgG, and bovine IgG were purchased from Beijing Boisynthesis Biotechnology Company. Bovine serum albumin (BSA) was purchased from Ding Guo Biotechnology Company (Beijing, China). Graphite was purchased from Sigma-Aldrich. 3-Mercaptopropinic acid (MPA), 2-mercaptoethylamine (MEA), 1-ethyl-3-(3-dimethylaminopropyl)carbodiimide (EDC) and N-hydroxysuccinimide (NHS) were purchased from Jkchemical. Hydrogen tetrachloroauratehydrate ($HAuCl_4 \cdot 3H_2O$) was purchased from Acrosl. Silver nitrate, cethltrimethlammonium bromide (CTAB), hydrogen peroxide, sodium borohydride, sodium hydroxide, acetic acid, ethanol, and all other chemicals were of analytical reagent grade. All the solutions were prepared with ultra pure water, and all the glasswares were cleaned with aqua regia before the experiments.

Bovine IgG, rabbit anti-transferrin and human IgG were stored at −20 °C and all other biological reagents were stored at 4 °C. Sodium phosphate buffered saline (PBS, 0.01 mol L^{-1}, pH 7.4) was used as running buffer.

2.2. Equipment

The wavelength modulation SPR analyzer installed in our laboratory was used (Wang et al., 2010). It is working with Kretschmann configuration to achieve the resonant condition by attenuated total reflection (ATR) in a prism. A 2 nm adhesive layer of Cr followed by a 50 nm layer of Au was deposited on a K9 glass slide (diameter: 2.4 cm; thickness: 0.7 mm; Jingpin Photoelectricity Company of Changchun, China), and then the glass slide with Au film was put on base of a prism (K9 glass, 2.7 cm × 1.9 cm × 1.9 cm; Jingpin Photoelectricity Company of Changchun, China) using a suitable index matching oil. A halogen tungsten lamp is used as the excitation light source. The light passes through a polarizer and two lenses and becomes TM-polarized parallel light. The parallel polychromatic light beam passes through the optical prism and excites surface plasmon at the interface between the Au film and the sample solution. The output light from another side of prism passes through the third optical focusing lens and the focusing spot size of area is 1.54 cm^2. One end of the optical fiber is put at the focal point of focusing lens and then the light beam has access to optical fiber as much as possible. The opposite end is connected to the spectrophotometer. Thus the output light is guided into the optical fiber and then enters the spectrophotometer (HR2000+, Ocean Optics Inc., USA). The HR2000+ spectrometer integrates a high-resolution optical bench, a powerful 2-MHz analog-to-digital (A/D) converter, programmable electronics, a 2048-element CCD-array detector and a high-speed USB 2.0 port. This combination produces extremely fast spectrometer and provides resolution to 0.035 nm (full width at half maximum, FWHM).

2.3. Synthesis of GO and AuNR–antibody conjugates

GO was prepared using a modification of Hummers and Offeman's method (1958) from graphite powders (Gilje et al., 2007). It was characterized using atomic force microscopy (AFM). AuNRs were chemically synthesized by a seed-mediated growth procedure (Jana et al., 2001; Nikoobakht and El-Sayed, 2003).

EDC/NHS linking chemistry was applied for the covalent attachment of antibodies onto AuNRs. 0.5 mL of 20 mmol L^{-1} MPA prepared in ethanol was added into 20 mL of AuNRs. The solution was kept under sonication for 1 h at 50 °C. Next, the AuNRs solution was centrifuged at 13,000 rpm for 30 min and the rod pellet was dissolved in 5.0 mL of ultra pure water. Then, 0.5 mL of a mixture of EDC and NHS (7.5 mmol L^{-1}:1.5 mmol L^{-1}) were added at room temperature. After 30 min, 0.1 mL of 500 μg mL^{-1} rabbit anti-transferrin was added into 0.025 mL of above solution followed by gently shaking for several seconds and kept for 1 h at 25 °C. Verification that biofunctionalized nanorod conjugates were prepared was confirmed using UV–vis spectroscopy.

2.4. Preparation of GO decorated with AuNR–antibody conjugates sensing substrate

The glass slide with Au film was fixed under the reactor. After PBS buffer was injected into the reactor, 10 mmol L^{-1} 2-mercaptoethylamine (MEA) was injected into the reactor and incubated for 1 h to form amino-modified Au film. Subsequently, 0.5 mg mL^{-1} GO was injected and assembled on the Au film via electrostatic interaction. Then the carboxyl groups of GO were activated with NHS (1.5 mmol L^{-1}) under the catalysis of EDC (7.5 mmol L^{-1}) for 25 min. PBS buffer was injected as the baseline solution. After the resonant wavelength kept constant, AuNR–antibody conjugates were injected into the reactor to covalently attach to the GO surface. After 12 h, PBS buffer was injected into the reactor to wash off unbound antibodies and to stabilize the baseline. Prior to the analysis, 10 mg mL^{-1} BSA was used to block the non-specific binding sites on the biosensor surface. A schematic diagram of the experimental procedure is shown in Fig. 1.

For traditional SPR biosensor substrate, 10 mmol L^{-1} MPA was injected into the reactor and incubated for 3 h. After –COOH group was activated with NHS (1.5 mmol L^{-1}) under the catalysis of EDC (7.5 mmol L^{-1}) for 25 min, the rabbit anti-transferrin was injected into the reactor. The following procedures were the same as that mentioned above.

2.5. Immunoassay

All SPR experiments were conducted at room temperature. After AuNR–antibody conjugates were immobilized on the surface of the biosensor, sample solution was separately injected into the reactor. After 40 min, PBS buffer was injected into the reactor. Due to a large amount of ions in the PBS, the antigen can be dissociated from the antibody immobilized on the surface of the biosensor and removed from the reactor by impulse injection of the PBS (Pei et al., 2000). After the antigen was removed from the reactor, another sample was introduced into the reactor. All experiments were conducted in triplicate to examine the reliability of the assays.

To evaluate the selective binding of transferrin, human IgG and bovine IgG were determined by the same procedure.

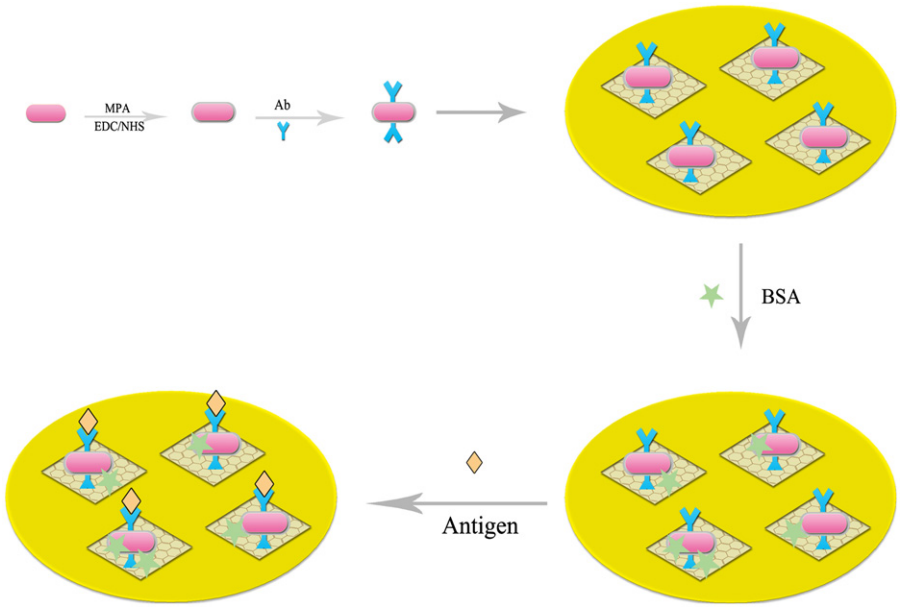

Fig. 1. A schematic diagram of experimental procedure. ( ) AuNRs, ( ) antibody, ( ) antigen, and ( ) GO sheets.

2.6. Regeneration

When the immunoassay was finished, the prism was taken away from the reactor. The glass slide was ultrasonically cleaned separately with ethanol and distilled water, and then dried with gaseous nitrogen. The Au film could be used repeatedly.

3. Results and discussions

3.1. Characterization of GO and AuNR–antibody conjugates

Water-soluble GO was synthesized by oxidizing graphite according to modified Hummer's method. Fig. 2 shows the tapping mode AFM image and histogram of the lateral dimensions distribution of isolated GO sheets. GO sheets have an average length of 210 ± 94 nm.

TEM images of AuNRs are shown in the inset of Fig. 3. The average length and width of the nanorods are 65 nm and 25 nm, respectively. The preparation of stable biofunctionalized AuNRs which interact specifically with their intended protein target is essential for enhanced SPR detection. Fig. 3 shows the UV–vis absorption spectra of as-prepared AuNRs, activated AuNRs, and AuNR–antibody conjugates in solution. The longitudinal band of the as-prepared purified AuNRs is observed at 738 nm as shown in Fig. 3 (curve a). When AuNRs were activated, this band is found to extend to 748 nm (curve b), which reflect the variation of the local dielectric function of activated AuNRs versus as-prepared AuNRs. A greater additional red-shift (776 nm; curve c) was observed upon exposing activated AuNRs to the excess amount of rabbit anti-transferrin solution (500 $\mu g\,mL^{-1}$, in PBS solution) for 1 h, which can be attributed to the change of localized refractive index near the AuNRs surface, indicating that the antibodies were successfully attached to the AuNRs surface. However, the transverse bands of AuNRs undergo almost no wavelength shift (curves a–c), which can be attributed to the fact that the longitudinal band more excellently responds to the binding to the target biomolecules in comparison with that of transverse band. It should be noted that the concentration of rabbit anti-transferrin used in our protocol is much higher than that of AuNRs solution in order to ensure a complete coverage of the AuNRs surface.

3.2. Preparation of GO decorated with AuNR–antibody conjugates sensing substrate

2-Mercaptoethylamine (MEA) can be attached strongly to the gold film surface by its sulfide bonds, and the amine terminal group lead to an amino-modified Au film which is positively charged. About 25 min later, the reaction of the MEA and gold film was completed and the maximum shift of resonance wavelength is 11.70 nm. Following this, after the amino-modified Au film was rinsed with PBS buffer, GO solution was flowed over MEA surface and completely assembled on the Au film in 30 min. The maximum shift of resonance wavelength is 7.20 nm for GO. Traditionally, SPR biosensor surface needs to be activated before immobilization and molecular self-assembly was used to form a sensing layer on Au film substrate. Here, GO with abundant oxygen-containing groups was used to immobilize AuNR–antibody conjugates. In the previous applications, GO was used as matrix for enzyme immobilization (Zhang et al., 2010). They demonstrated that the enzyme immobilization on the GO sheets could take place readily without additional surface modification and the maximum loading of enzyme is much higher than the loadings on many reported materials. Because of the large surface area in low manufacturing cost of the GO and its interaction with the target molecules, this enrichment can also be utilized to enhance the sensitivity of the biomolecules detection. The surface of GO was functionalized with different kinds of oxygen-containing functional groups such as carboxyl, epoxy, and hydroxyl groups. After the GO sheets were assembled on amino-modified Au film, the carboxyl groups were further activated by EDC/NHS. This is a universal technique to conjugate carboxyl to amine groups in peptides and proteins. EDC reacts with a carboxylic acid to form an amine-reactive intermediate. Then, in the presence of NHS, the amine-reactive intermediate can be converted to amine-reactive NHS esters. As a result, AuNR–antibody conjugates could be immobilized on the GO layers through covalent attachment between the amine groups of antibodies and the activated carboxyl groups of GO sheets (Jung et al., 2010). The AuNRs covered with antibodies were adsorbed on the GO surface using antibodies as novel linkage. Meanwhile, the GO sheets decorated with AuNR–antibody conjugates exhibit specific detection of antigen. In this process, a small portion of antibodies act as linkage between the

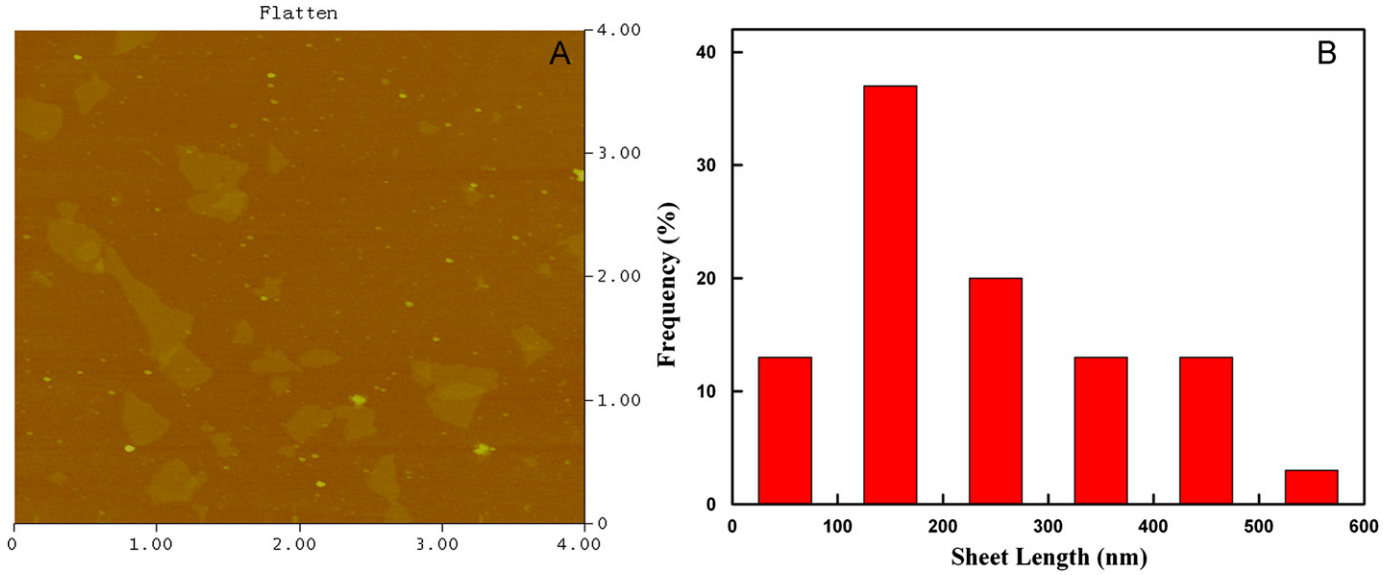

Fig. 2. Tapping mode AFM image (A) and histogram of the lateral dimensions distribution of isolated GO sheets (B).

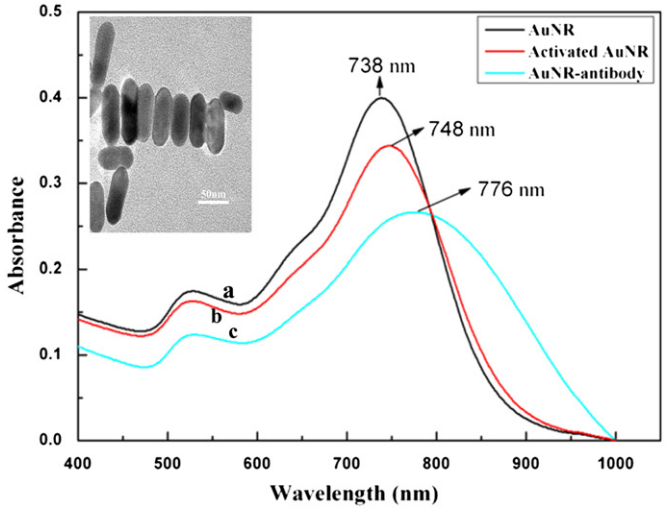

Fig. 3. UV–vis absorption spectra of AuNRs (a), activated AuNRs (b) and AuNR–antibody conjugates (c). Inset shows TEM images of AuNRs.

GO sheets and AuNRs. These antibodies may lose their functional capacity for specific interaction with antigen. Though it is difficult to evaluate how much functional capacity is lost, the AuNRs covered with numerous antibodies have a stereo structure and most of the antibodies still retain their reaction activity toward antigen except for the small quantity of antibodies on the junction surface. Compared with conventional Au film substrate, the three dimensional GO–AuNR substrate has a larger capacity for antibody immobilization, which is beneficial to antigen detection. In order to select the optimum concentration of antibody, AuNR–antibody conjugates at different concentrations of rabbit anti-transferrin were separately injected into the reactor. The effect of the concentration of rabbit anti-transferrin on the shift of the resonant wavelength is also shown in Fig. 4A. With the increase of the concentration of AuNR–antibody conjugates, more conjugates were immobilized on the biosensor surface, resulting in the resonant wavelength moving to the longer wavelength. The maximum resonant wavelength shifts for the immobilization of AuNR–antibody conjugates at concentrations of 125 and 150 μg mL^{-1} are almost the same. Relatively high concentration of antibodies might result in stereo hindrance. Therefore, 125 μg mL^{-1} instead of 150 μg mL^{-1} was chosen as the optimum concentration for the detection of transferrin. It is reasonable that the present substrate immobilized more antibodies for antigen detection because of the three dimensional GO–AuNR substrate compared with conventional Au film substrate. As shown in Fig. 4A, when the concentration of rabbit anti-transferrin is 125 μg mL^{-1}, the maximum resonant wavelength shift for the immobilization of AuNR–antibody conjugates is 20.40 nm within 60 min.

In order to evaluate the effect of the fabricated substrate on performance of SPR biosensor, the traditional substrate based on Au film was also investigated. The kinetic adsorption curve of 125 μg mL^{-1} rabbit anti-transferrin obtained with the SPR biosensor based on Au film is also shown in Fig. 4A. The maximum shift of the resonant wavelength is 7.90 nm for traditional Au film, while it is 20.40 nm for present substrate. When the GO–AuNR–antibody structures were used, the signal was dramatically enhanced. The large surface area and high loading capacity for biomolecules of GO are beneficial to the conjugates immobilization. Compared with traditional Au film substrate, the stereo substrate of GO–AuNR–antibody structures provides a high capability for antibody immobilization, which also exhibits superb accessibility for the target protein to enhance its sensing performance significantly. AuNRs immobilized on GO surface lead to large resonant wavelength shift and function as sensitivity enhancers in immunoassay.

3.3. Determination of transferrin

To demonstrate the potential sensitivity of SPR biosensor based on GO decorated with AuNR–antibody conjugates substrate, transferrin at different concentrations was separately injected into the reactor at room temperature. The shifts of resonant wavelength due to antibody–antigen immunoreaction were measured in real time. Fig. 4B shows the relationship between the shifts in the resonant wavelength and the concentrations of transferrin. Fig. 5 shows the SPR spectrum for detection of 10 μg mL^{-1} transferrin in different methods. The curve a in Fig. 5 is the SPR spectrum when the biosensor surface was washed with PBS buffer until the resonant wavelength kept constant after the antibody immobilization and BSA blocking. Under the same concentration of rabbit anti-transferrin, GO decorated with AuNR–antibody conjugates substrate causes

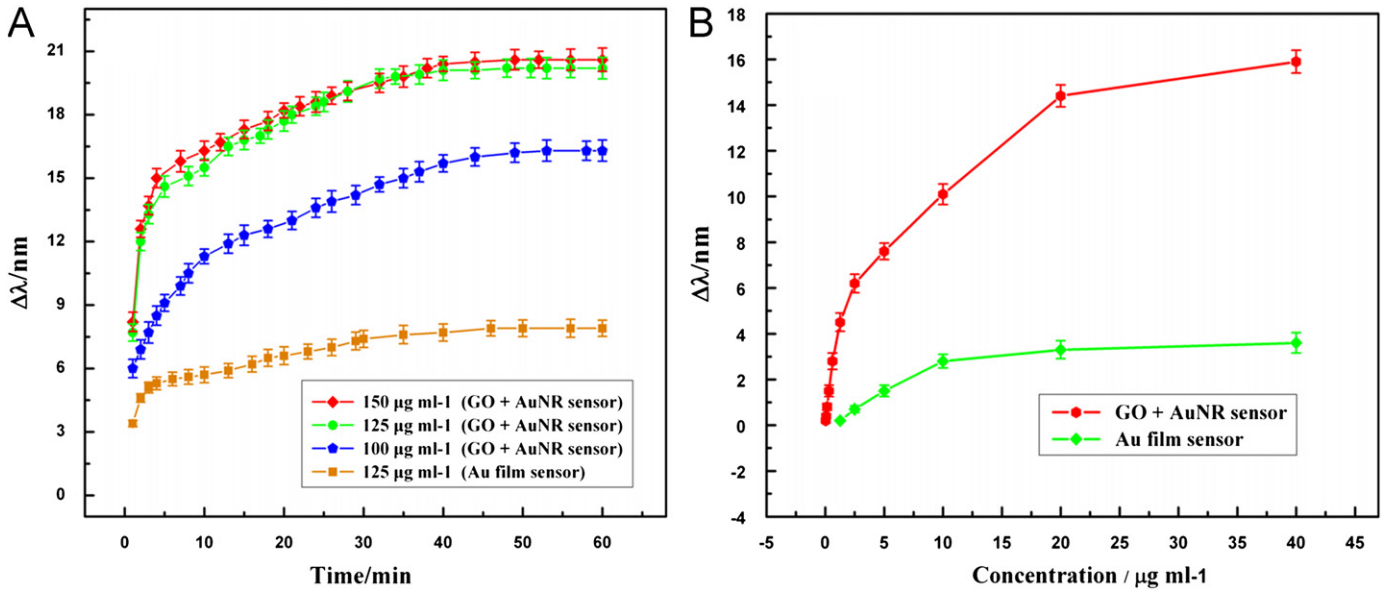

Fig. 4. The kinetic adsorption curves of rabbit anti-transferrin obtained with SPR biosensor at different rabbit anti-transferrin concentration (A) and the relationship between the shifts of the resonant wavelength and the concentrations of transferrin (B).

the shift of resonant wavelength toward longer wavelength (660.2 nm in Fig. 5B). The red-shift of resonant wavelength in some wavelength range is also beneficial to the sensitivity of wavelength modulation SPR biosensor (Homola, 1997; Homola et al., 1999). Incubation of an antibody-modified Au film with 10 μg mL^{-1} solution of transferrin yields 2.7 nm shift in resonant wavelength (Fig. 5A). While the exposure of GO decorated with AuNR–antibody conjugates to 10 μg mL^{-1} solution of transferrin results in 10.2 nm shift in resonant wavelength (Fig. 5B). The significant increase in signal of the interaction between anti-transferrin and transferrin was afforded through the use of GO decorated with AuNR–antibody conjugates substrate in this scheme. As a result, the SPR biosensor based on GO decorated with AuNR–antibody conjugates shows a good response to transferrin in the concentration range of 0.0375–40.00 μg mL^{-1}. The minimum shift of resonant wavelength is 0.20 nm at 0.0375 μg mL^{-1} and the maximum shift is 15.90 nm at 40.00 μg mL^{-1}. The SPR biosensor based on Au film substrate shows a response to transferrin in the concentration range of 1.25–40.00 μg mL^{-1}. The shift of resonant wavelength is 0.20 nm at 1.25 μg mL^{-1} and 3.60 nm at 40.00 μg mL^{-1}.

With the increase of concentration of transferrin, the binding sites of the antibodies immobilized on the surface will be saturated. When the concentration of the transferrin was higher than 40 μg mL^{-1}, no further obvious shift of the resonant wavelength was observed and this concentration is the upper determination limit. The detected minimum resonant wavelength shift of the SPR biosensor installed in our laboratory is 0.20 nm, and the lowest concentration of the antigen that can be detected is determined by the minimum shift of resonant wavelength. Under identical conditions, the lowest concentration that can be detected with the GO–AuNR–antibody substrate is 0.0375 μg mL^{-1}, which is 32 times lower than that obtained with conventional Au film. The wavelength modulation SPR biosensor based on staphylococcal protein A and colloidal Au-amplified assay for determination of transferrin has a response in the concentration range of 0.05–20 μg mL^{-1} (Liu et al., 2006). The lowest concentration detected by present biosensor is lower than the previous report and the upper determination limit is expanded to 40 μg mL^{-1}. As mentioned above, the experimental results indicated that the performance of the wavelength-modulation SPR biosensor based on GO decorated with AuNR–antibody conjugates substrate was significantly improved.

The specificity is demonstrated by detecting human IgG and bovine IgG under the same conditions (Mayer et al., 2008; Lyon et al., 1998). After the rabbit anti-transferrin was immobilized on the surface of the biosensor, human IgG and bovine IgG at the concentrations of 10 μg mL^{-1} were separately injected into the reactor for 40 min. There are no observable shifts of the resonant wavelength (Fig. 5), which indicates the selective binding of transferrin. The biosensor retains the specificity of antigen. However, this type of biosensor could be used for detecting various proteins by decorating GO sheets with corresponding AuNR–antibody conjugates such as rabbit anti-human IgG for human IgG detection.

A GO-based detection platform has several advantages for optical sensing of biomolecules compared with conventional molecular beacons. The two-dimensional sheet is equipped with a range of functional groups that can interact in an ionic, covalent or non-covalent manner, so that in principle it provides the highest extraction efficiencies of biomolecules per unit area of virtually any material (Loh et al., 2010). Here, AuNR–antibody conjugates were assembled on the GO surface for specific detection of antigen. The high water solubility, large surface area and high loading capacity for target biomolecules of GO are beneficial to the antibody immobilization of SPR biosensor. AuNRs exhibit two absorption bands: one is the transverse band, corresponding to electron oscillation along the short axis of AuNRs; and the other is the longitudinal band, corresponding to electron oscillation along the long axis of AuNRs. The nanorods have their own localized surface plasmon resonance and can change the SPR features of the substrate. The electronic coupling between AuNRs and the surface plasmon wave leads to the amplification of the SPR response originating from the dielectric changes of the substrate upon binding of the antigen–antibody complexes. Moreover, when AuNRs were anchored to the GO surface using antibodies as novel linkage, the optical and electronic properties of the substrate changed. The surface plasmon of AuNRs might be resonantly excited through energy transfer in the near field and create a strong local electromagnetic field, which further enhanced the shift of resonant wavelength. The thickness of the sensing membrane increases and the resonant wavelength moves to longer wavelength, which also leads to the sensitivity enhancement of the wavelength-modulation SPR biosensor.

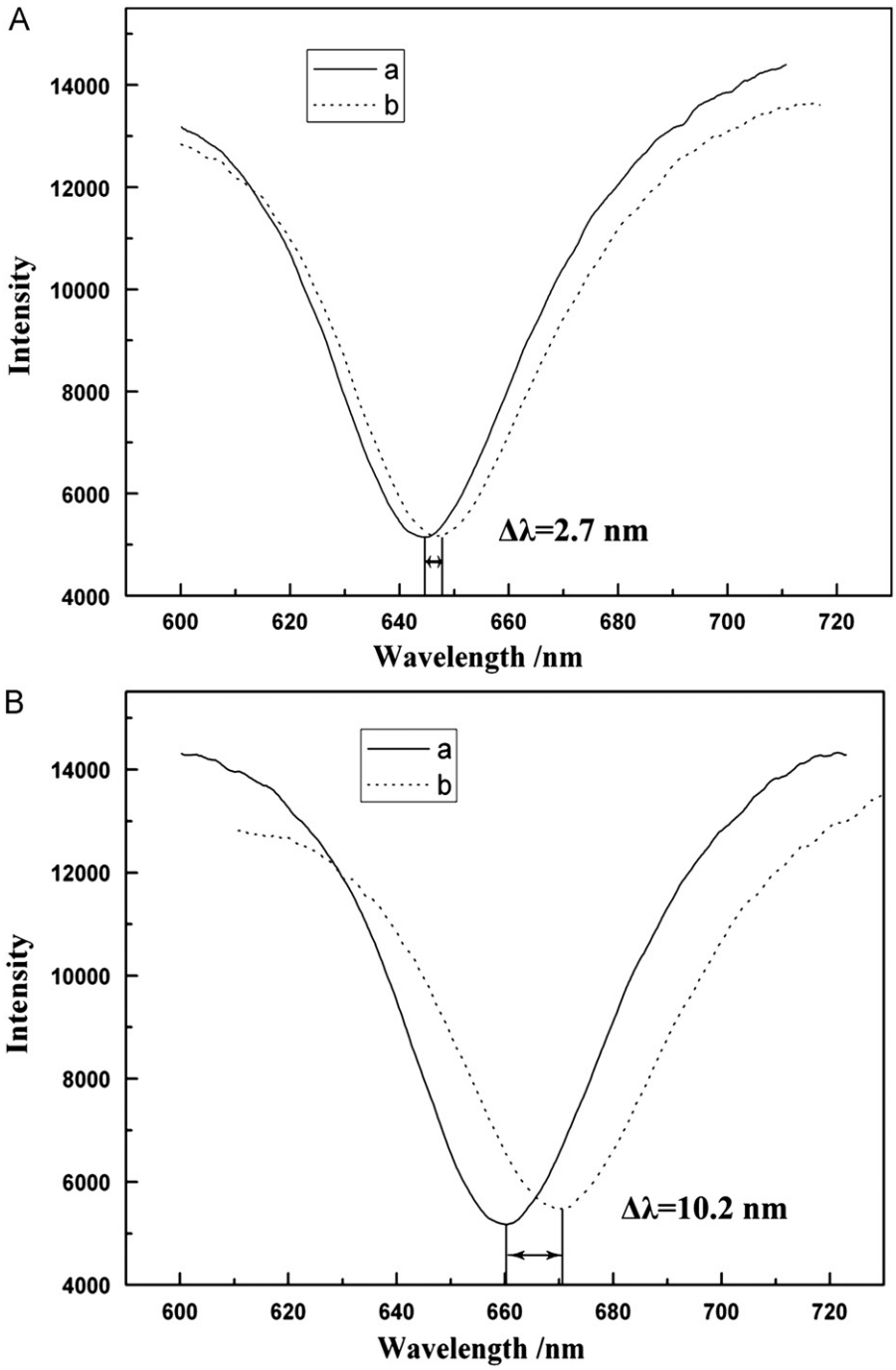

Fig. 5. The SPR spectrum for detection of transferrin at the concentration of 10 μg mL^{-1} in different methods: detection based on traditional Au film (A) and detection based on GO decorated with AuNR–antibody conjugates (B).

The experimental results demonstrate that the use of GO decorated with AuNR–antibody conjugates sensing substrate in SPR biosensor significantly permitted the enhancement in the lowest concentration that can be detected.

3.4. Calculation of binding constant K_A

For 1:1 reaction of antigen (Ag) and antibody (Ab): Ag + Ab = AgAb, the binding constant is K_A (Stěpánek et al., 2006).

$$K_A = \frac{[AgAb]}{[Ag][Ab]} \quad (1)$$

The association phase of the interaction kinetics measured as SPR signal can be expressed as (Sun et al., 2006)

$$\frac{d\Delta\lambda}{dt} = ka[Ag]\,(\Delta\lambda_{max} - \Delta\lambda) - k_d\Delta\lambda \quad (2)$$

where $d\Delta\lambda/dt$ is the rate of the change of SPR response, [Ag] is the concentration of antigen in the solution, k_a and k_d are association and dissociation rate constants, respectively. $\Delta\lambda_{max}$ is a constant for a special sensing membrane, which is corresponding to the maximum capacity of binding antigen on the sensor surface. $\Delta\lambda$ is the bound antigen measured as the biosensor response at time t. At equilibrium, the signal reached a plateau and $\Delta\lambda$ should be expressed as $\Delta\lambda_{eq}$, then $d\Delta\lambda eq/dt = 0$. According to $K_A = k_a/k_d$,

Eq. (2) becomes

$$\frac{\Delta\lambda_{eq}}{[Ag]} = K_A\Delta\lambda_{max} - K_A\Delta\lambda_{eq} \quad (3)$$

A plot of $\Delta\lambda$eq/[Ag] against $\Delta\lambda_{eq}$ can be used to obtain K_A from the slope of the plot. Here the binding constant of transferrin with antibody is $1.65\times10^7\ L^{-1}$ mol based on proposed biosensor and $1.49\times10^7\ L^{-1}$ mol based on traditional biosensor. The curve of relationship between the shifts of the resonant wavelength and the concentrations of transferrin based on proposed biosensor has a R^2 value of 0.7954. The shift of the resonant wavelength does not linearly increase with the increase of the concentration of transferrin in certain concentration range. $\Delta\lambda_{eq}$ increases with the increase of concentration of antigen ([Ag]) in the solution. It is seen from Eq. (3) that the $\Delta\lambda_{eq}$/[Ag] decreases with the increase of $\Delta\lambda_{eq}$. So the slope of the relationship curve between the shift of the resonant wavelength and the concentration of transferrin decreases with the increase of the concentration of antigen, which is in accordance with the experimental results.

4. Conclusions

In summary, a new strategy for effective immobilization of antibody and sensitivity enhancement of SPR biosensor is presented. The immunosensor based on GO sheets decorated with AuNR–antibody conjugates shows a satisfactory response to transferrin in the concentration range of 0.0375–40.00 μg mL^{-1}. Combination of the high loading capacity for target biomolecules of GO with high sensitivity of AuNRs has been demonstrated to be beneficial for the improvement of the performance of SPR biosensor. It is anticipated that this sensor can be used for detecting various proteins by decorating GO sheets with selected AuNR–antibody conjugates, which makes the new sensor capable of detecting a variety of proteins and provides a promising potential for manufacturing other sensitive biosensors. However, the proposed design has not been applied in practical detection and the present sensitivity could be further improved by optimizing the device structure and exploring more types of Au particles. Nanoparticles with sharp tips and high sensitivity will be used to modify the GO sheets such as triangular Au nanoplates and Au bipyramids to improve sensitivity within the framework of the proposed design in future.

Acknowledgments

This work was supported by National Natural Science Foundation of China (Nos. 20727003, 21075049, and 21105037), Program for New Century Excellent Talents in University (No. NECT-10-0443), Special-funded Programme on National Key Scientific Instruments and Equipment Development (No. 2012YQ090194) and Science and Technology Developing Foundation of Jilin Province (Nos. 20100356, and 20110162).

Appendix A. Supporting information

Supplementary data associated with this article can be found in the online version at http://dx.doi.org/10.1016/j.bios.2013.02.008.

References

Asobayire, F.S., Adou, P., Davidsson, L., Cook, J.D., Hurrell, R.F., 2001. American Journal of Clinical Nutrition 74, 776–782.
Bilitewski, U., 2000. Analytical Chemistry 72, 692A–701A.
Boukhvalov, D.W., Katsnelson, M.I., 2008. Journal of the American Chemical Society 130, 10697–10701.
Cai, L.P., Zhan, R.Y., Pu, K.Y., Qi, X.Y., Zhang, H., Huang, W., Liu, B., 2011. Analytical Chemistry 83, 7849–7855.
Chang, C.-C., Lin, S.H., Wei, S.-C., Chen, C.Y., Lin, C.W., 2011. Biosensors and Bioelectronics 30, 235–240.
Chang, Y.R., Li, H.Y., Chen, K., Chang, C.C., Tsai, D.S., Fu., C.C., Tzeng, Y.K., Fang, C.Y., Han, C.C., Chang, H.C., Fan, W., 2008. Nature Nanotechnology 3, 248–288.
Daniel, M.C., Astruc, D., 2004. Chemical Reviews 104, 293–346.
Das, G.A., Abbi, A., 2003. American Journal of Hematology 72, 158–161.
Dong, H.F., Gao, W.C., Yan, F., Ji, H.X., Ju, H.X., 2010a. Analytical Chemistry 82, 5511–5517.
Gilje, S., Han, S., Wang, M., Wang, K.L., Kaner, R.B., 2007. Nano Letters 7, 3394–3398.
He, Q.Y., Sudibya, H.G., Yin, Z.Y., Wu, S.X., Li, H., Boey, F., Huang, W., Chen, P., Zhang, H., 2010. ACS Nano 4, 3201–3208.
He, S.J., Song, B., Li, D., Zhu, C.F., Qi, W.P., Wen, Y.Q., Wang, L.H., Song, S.P., Fang, H.P., Fan, C.H., 2010. Advanced Functional Materials 20, 453–459.
Homola, J., 1997. Sensors and Actuators B 41, 207–211.
Homola, J., 2008. Chemical Reviews 108, 462–493.
Homola, J., Koudela, I., Yee, S.S., 1999. Sensors and Actuators B 54, 16–24.
Hu, W.H., Lu, Z.S., Liu, Y.S., Li, C.M., 2010. Langmuir 26, 8386–8391.
Hummers, W.S., Offeman, R.E., 1958. Journal of the American Chemical Society 80, 1339.
Jana, N.R., Gearheart, L., Murphy, C.J., 2001. Advanced Materials 13 (18), 1389–1393.
Jung, J.H., Cheon, D.S., Liu, F., Lee, K.B., Seo, T.S., 2010. Angewandte Chemie International Edition 49, 5708–5711.
Liu, X., Sun, Y., Song, D.Q., Zhang, Q.L., Tian, Y., Zhang, H.Q., 2006. Talanta 68, 1026–1031.
Loh, K.P., Bao, Q.L., Eda, G., Chhowalla, M., 2010. Nature Chemistry 2, 1014–1015.
Lyon, L.A., Musick, M.D., Natan, M.J., 1998. Analytical Chemistry 70, 5177–5183.
Mayer, K.M., Lee, S., Liao, H.W., Rostro, B.C., Fuentes, A., Scully, P.T., Nehl, C.L., Hafner, J.H., 2008. ACS Nano 2, 687–692.
Nikoobakht, B., El-Sayed, M.A., 2003. Chemistry of Materials 15 (10), 1957–1962.
Parab, H.J., Jung, C., Lee, J.H., Park, H.G., 2010. Biosensors and Bioelectronics 26, 667–673.
Pei, R., Cui, X., Yang, X., Wang, E., 2000. Talanta 53, 481–488.
Pernites, R.B., Ponnapati, R.R., Advincula, R.C., 2010. Macromolecules 43, 9724–9735.
Ren, W., Fang, Y.X., Wang, E.K., 2011. ACS Nano 5, 6425–6433.
Satishkumar, B.C., Brown, L.O., Gao, Y., Wang, C.-C., Wang, H.-L., Doorn, S.K., 2007. Nature Nanotechnology 2, 560–564.
Sun, Y., Bai, Y.P., Song, D.Q., Li, X.Z., Wang, L.Y., Zhang, H.Q., 2007. Biosensors and Bioelectronics 23, 473–478.
Sun, Y., Liu, X., Song, D.Q., Tian, Y., Bi, S., Zhang, H.Q., 2006. Analytica Chimica Acta 569, 21–26.
Singh, V.V., Gupta, G., Batra, A., Nigam, A.K., Boopathi, M., Gutch, P.K., Tripathi, B.K., Srivastava, A., Samuel, M., Agarwal, G.S., Singh, B., Rajagopalan, Vijayaraghavan, 2012. Advanced Functional Materials 22, 2352–2362.
Stěpánek, J., Vaisocherova, H., Piliarik, M., 2006. Springer Series on Chemical Sensors and Biosensors 4, 69–91.
Wang, J., Wang, L.Y., Sun, Y., Zhu, X.N., Cao, Y.B., Wang, X.H., Zhang, H.Q., Song, D.Q., 2010. Colloids and Surfaces B: Biointerfaces 75, 520–525.
Wang, T., Zhang, S.Y., Mao, C.J., Song, J.M., Niu, H.L., Jin, B.K., Tian, Y.P., 2012. Biosensors and Bioelectronics 31, 369–375.
Wen, Y.Q., Xing, F.F., He, S.J., Song, S.P., Wang, L.H., Long, Y.T., Li, D., Fan, C.H., 2010. Chemical Communications 46, 2596–2598.
Zhang, J.L., Zhang, Feng, Yang, J., Huang, X.L., Liu, H., Zhang, J.Y., Guo, S.W., 2010. Langmuir 26 (9), 6083–6085.